THE JOURNAL OF BIOLOGICAL CHEMISTRY
Vol. 277, No. 26, Issue of June 28, pp. 23469–23476, 2002

Printed in U.S.A.

The FeMoco-deficient MoFe Protein Produced by a *nifH* Deletion Strain of *Azotobacter vinelandii* Shows Unusual P-cluster Features*

Received for publication, March 1, 2002, and in revised form, April 23, 2002
Published, JBC Papers in Press, April 26, 2002, DOI 10.1074/jbc.M202061200

Markus W. Ribbe‡§, Yilin Hu‡, Maolin Guo‡, Benedikt Schmid¶, and Barbara K. Burgess‡†

From the ‡Department of Molecular Biology and Biochemistry and the Program in Macromolecular Structure, University of California, Irvine, California 92697-3900 and ¶Division of Chemistry and Chemical Engineering, California Institute of Technology, Pasadena, California 91125

The His-tag MoFe protein expressed by the *nifH* deletion strain *Azotobacter vinelandii* DJ1165 (Δ*nifH* MoFe protein) was purified in large quantity. The $\alpha_2\beta_2$ tetrameric Δ*nifH* MoFe protein is FeMoco-deficient based on metal analysis and the absence of the S = 3/2 EPR signal, which arises from the FeMo cofactor center in wild-type MoFe protein. The Δ*nifH* MoFe protein contains 18.6 mol Fe/mol and, upon reduction with dithionite, exhibits an unusually strong S = 1/2 EPR signal in the g ≈ 2 region. The indigo disulfonate-oxidized Δ*nifH* MoFe protein does not show features of the P^{2+} state of the P-cluster of the Δ*nifB* MoFe protein. The oxidized Δ*nifH* MoFe protein is able to form a specific complex with the Fe protein containing the $[4Fe\text{-}4S]^{1+}$ cluster and facilitates the hydrolysis of MgATP within this complex. However, it is not able to accept electrons from the $[4Fe\text{-}4S]^{1+}$ cluster of the Fe protein. Furthermore, the dithionite-reduced Δ*nifH* MoFe can be further reduced by Ti(III) citrate, which is quite unexpected. These unusual catalytic and spectroscopic properties might indicate the presence of a P-cluster precursor or a P-cluster trapped in an unusual conformation or oxidation state.

The metalloenzyme nitrogenase complex catalyzes the biological reduction of dinitrogen to ammonia (for recent reviews, see Refs. 1–6). The enzyme is composed of two separately purifiable proteins, the iron (Fe) protein and the molybdenum-iron (MoFe)[1] protein. The Fe Protein is a 60-kDa dimer of two identical subunits encoded by the *nifH* gene. The two subunits are bridged by a [4Fe-4S] cluster, and each subunit has a binding site for MgATP. The more complicated MoFe protein is a 230-kDa $\alpha_2\beta_2$ tetramer with the α and β subunits encoded by the *nifD* and *nifK* genes, respectively. The MoFe protein contains two different types of metal clusters, the [8Fe-7S] cluster (P-cluster) bridged between each $\alpha\beta$ subunit pair and the [Mo-7Fe-9S-homocitrate] cluster (FeMoco) located within each α subunits. Substrate reduction by the enzyme requires both component proteins, with the Fe protein serving as a specific reductant of the MoFe protein, which in turn provides the site of substrate reduction. To carry out the catalytic function of nitrogenase, the reduced Fe protein first binds two molecules of MgATP and undergoes a conformational change before forming a complex with the MoFe protein. Then, coupled with MgATP hydrolysis, electrons are transferred from the Fe protein to the P-clusters of the MoFe protein within the complex. This process is followed by the dissociation and re-reduction of the oxidized Fe protein and the dissociation of MgADP from the MoFe protein. Finally, the electrons are believed to be transferred from the P-cluster to the FeMoco, where substrate reduction occurs.

FeMoco-deficient, but P-cluster containing MoFe proteins have proved to be useful for the study of two major aspects of the nitrogenase research, the maturation of MoFe protein (7–18) and the features of the P-cluster (10, 19–21). Two types of 100% FeMoco-deficient MoFe proteins, presumably different catalytically and structurally, have been isolated and characterized. One was expressed by a *nifB* deletion strain (12, 21–22), and the other was expressed by a *nifH* deletion strain (10). The *nifB* gene product (NifB) is involved in the synthesis of the FeMoco (23), a process independent of the production of the MoFe protein polypeptides (24–26). NifB produces an iron- and sulfur-containing FeMoco precursor, NifB-co, presumably the starting point of the FeMoco synthesis (23). In addition, FeMoco synthesis in *Azotobacter vinelandii* also requires the Fe protein, reductant, MgATP, a protein designated γ (15), and the combined action of at least five more *nif* gene products, including *nifN*, *nifE*, *nifX*, *nifQ*, and *nifV* (for reviews, see Refs. 27–34 and 35). The Fe protein is involved not only in the biosynthesis of FeMoco but also in the insertion of preformed FeMoco into a FeMoco-deficient form of the MoFe protein during the final maturation of the holo-MoFe protein (27–34). This maturation process most likely occurs in a series of steps. Initially the FeMoco site is inaccessible to FeMoco insertion (7–9). The conversion to another form with the FeMoco site accessible for FeMoco insertion involves at least the Fe protein, GroEL, MgATP, and γ (9, 11–15, 18). All required components for this conversion are available *in vivo* in *nifB* deletion strains. Therefore, this step has already occurred and the FeMoco-deficient MoFe protein that accumulates in this strain (Δ*nifB* MoFe protein) has the FeMoco site in an open conformation and can be directly activated with isolated FeMoco (9). In contrast, the conversion to an accessible FeMoco binding site cannot occur in the absence of Fe protein, which is the case in the *nifH* deletion strain. Consequently, MoFe proteins produced by *nifH* deletion strains (Δ*nifH* MoFe protein) of *A. vinelandii*, such as DJ54, have the FeMoco site in a closed conformation (7–10).

Earlier studies suggested that the Δ*nifB* and Δ*nifH* MoFe proteins are different in not only the conformations of their FeMoco binding sites but also their P-cluster features (10, 21).

* This work was supported by National Institutes of Health Grant GM-43144 (to B. K. B.). The costs of publication of this article were defrayed in part by the payment of page charges. This article must therefore be hereby marked "*advertisement*" in accordance with 18 U.S.C. Section 1734 solely to indicate this fact.

We dedicate this paper to Professor Barbara K. Burgess for her ingenious contribution to this work.

§ To whom correspondence should be addressed: Dept. of Molecular Biology and Biochemistry, University of California, Irvine, CA 92697. Tel.: 949-824-4737; Fax: 949-824-8551; E-mail: markus@nitrolab.bio.uci.edu or ribb111@yahoo.com.

† Deceased December 29, 2001.

[1] The abbreviations used are: MoFe, molybdenum-iron; IDS, indigo disulfonate.

The exact function and redox properties of the P-cluster have been the focus of discussion for a long time (2). Which oxidation states of the P-cluster are required in the process of electron transfer from the Fe protein to the FeMoco of the MoFe protein still remain controversial, and several possibilities have been suggested. Some favor the theory that involves two-electron oxidized P^{OX} states or at least states more oxidized than P^N, the dithionite-reduced state of the P-cluster (36, 37), where others favor redox states more reduced than P^N (2, 19). A comparative study of the Δ*nifB* and Δ*nifH* MoFe proteins can be used to address this problem as well as many other remaining questions about the function and assembly of the P-cluster. However, the instability of these FeMoco-deficient MoFe proteins and the loss of protein activity during the time-consuming purification procedure prevented reasonable protein yields for subsequent experiments. Recently, an efficient one step purification of a His-tag version of the Δ*nifB* MoFe protein has been reported that allowed the isolation of a sufficient amount of protein for further studies (21). Here we report a detailed catalytic and biophysical characterization of Δ*nifH* MoFe protein using the same expression and purification strategies for this mutant protein.

EXPERIMENTAL PROCEDURES

Unless otherwise noted, all chemicals and reagents were obtained from Fisher, Baxter Scientific, or Sigma.

Construction of the Variant A. vinelandii Strain, Cell Growth, and Protein Purification—*A. vinelandii* Δ*nifH* mutant strain DJ1165, expressing a FeMoco-deficient His-tag MoFe protein (Δ*nifH* MoFe protein), was constructed by transforming competent cells of *A. vinelandii* DJ1141 with plasmid pDB115, which contained the *nifH* gene with a deletion within its coding sequence. The successful transformation of *A. vinelandii* strain DJ1141 by pDB115 was confirmed by the inability of the transformed cells to grow without a source for nitrogen fixation. The resulting *A. vinelandii* DJ1165 contains an in-frame deletion within the *nifH* gene, extending from codon 158 to 200. The construction of plasmid pDB115 (38) and *A. vinelandii* strain DJ1141 (21) has been described elsewhere. The FeMoco-deficient His-tag MoFe protein expressed by *A. vinelandii* DJ1143 is designated as Δ*nifB* MoFe protein, and the construction of *A. vinelandii* DJ1143 has been reported in details previously (21).

A. vinelandii mutant strains DJ1165, DJ1143, CA12 (Δ*nifHDK*), and wild type were grown in 180-liter batches in a 200-liter New Brunswick fermentor on Burke's minimal medium supplemented with 2 mM ammonium acetate. The growth rate was measured by cell density at 436 nm using a Spectronic 20 Genesys (Spectronic Instruments, Rochester, NY). After the consumption of the ammonia, the cells were de-repressed for 3 h followed by harvesting using a flow-through centrifugal harvester (Cepa). The cell paste was washed with 50 mM Tris-HCl (pH 8.0) and kept on dry ice until needed.

Published methods were used for the purification of wild-type Fe protein (39), wild-type MoFe protein (40), Δ*nifB* MoFe protein (21), and the preparation of crude extract of *A. vinelandii* strain CA12 (18). Δ*nifH* MoFe protein was purified as described for the Δ*nifB* MoFe protein (21) using a slight modification. All buffers contained 10% glycerol.

Protein Characterization and Spectroscopy—All spectroscopic samples were prepared in a vacuum atmosphere dry box with an oxygen level of less than 4 ppm. Unless noted otherwise, all samples were in 25 mM Tris·HCl (pH 8.0), 10% glycerol, and 2 mM $Na_2S_2O_4$. MoFe protein samples were oxidized by the addition of excess of indigo disulfonate (IDS) and incubated for 30 min. Subsequently, indigo disulfonate was removed by a single passage over an anion-exchange column as described elsewhere (41). Ti(III) citrate and the Ti(III) citrate-reduced samples were prepared according to published methods (42, 43). Ti(III) citrate, like $Na_2S_2O_4$, was removed on a Sephadex G-25 column. Samples were either used as they were or they were concentrated in a Centricon-30 (Amicon) concentrator in anaerobic centrifuge tubes outside the dry box. For UV-visible absorption experiments samples were prepared in anaerobic cuvettes that were previously blanked. Spectra were recorded on an HP 8452A diode array spectrophotometer. All perpendicular and parallel mode EPR spectra were recorded using a Bruker ESP 300 E_z spectrophotometer interfaced with an Oxford Instruments ESR-9002 liquid helium continuous flow cryostat. All spectra were recorded at 10 K using a microwave power of 50 mW, a gain of 5×10^4, a modulation frequency of 100 kHz, and a modulation amplitude of 5 G. The microwave frequencies of 9.62 and 9.39 GHz were used for the perpendicular (10 scans)- and parallel (20 scans)-mode EPR spectra, respectively.

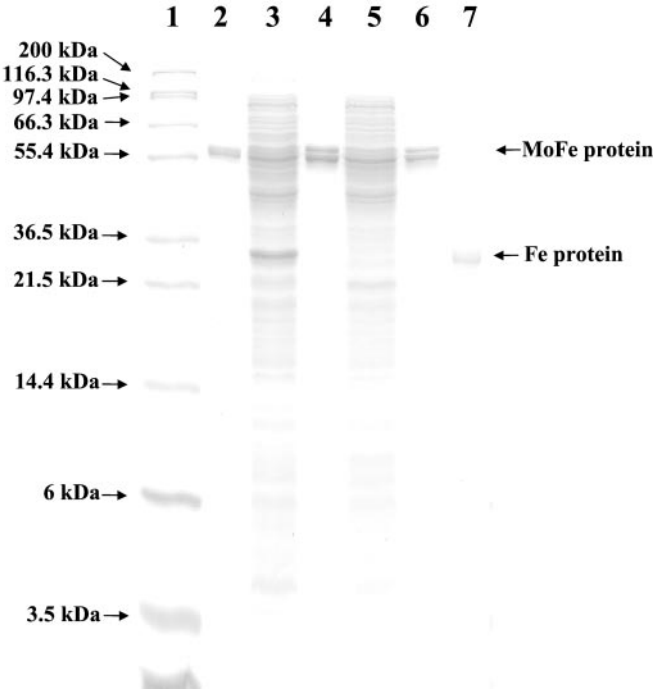

FIG. 1. **Coomassie-stained SDS-polyacrylamide gel electrophoresis of purified Δ*nifH* and Δ*nifB* MoFe protein.** *Lane 1*, protein standard, 15 μg; *lane 2*, purified wild-type MoFe protein, 5 μg; *lane 3*, crude extract of *A. vinelandii* DJ1143 (Δ*nifB* His-tag MoFe protein strain), ~20 μg; *lane 4*, purified His-tag Δ*nifB* MoFe protein, 5 μg; *lane 5*, crude extract of *A. vinelandii* DJ1165 (Δ*nifH* His-tag MoFe protein strain), ~20 μg; *lane 6*, purified His-tag Δ*nifH* MoFe protein, 5 μg; *lane 7*, purified wild-type Fe protein, 2 μg. A molecular weight of 23,000–26,000 was reported for the monomeric γ protein based on SDS-PAGE (15). The molecular weights of the native wild type and the His-tag Δ*nifH* MoFe proteins appeared to be identical based on the elution profiles of both proteins on a gel filtration Sephacryl S-200 HR column (Amersham Biosciences).

All nitrogenase activity assays (8.7-ml vials) were carried out as described previously (40). The products H_2 and C_2H_4 were analyzed as published elsewhere (44). Ammonium was determined by a high performance liquid chromatography fluorescence method (45). Phosphate was analyzed as described elsewhere (46). Molybdenum (47) and iron (48) were determined as published elsewhere. The iron-chelating assays were performed as described elsewhere (43) using a Fe protein concentration of 0.8 mg/ml.

Reconstitution Assays—The assays designed to reconstitute pure Δ*nifH* MoFe protein contained 25 mM Tris·HCl (pH 8.0), 10% glycerol, 0.5 M NaCl, 0.85 mM ATP, 1.7 mM $MgCl_2$, 10 mM creatine phosphate, 11 units of creatine kinase, 20 mM $Na_2S_2O_4$, 1.5 mg wild-type Fe protein, 1 mg of pure Δ*nifH* MoFe protein, and up to 50 mg of crude extract of *A. vinelandii* CA12 (*nifHDK*) in a 1.0-ml total volume. The insertion was started by the addition of isolated FeMoco in *N*-methylformamide. The samples were incubated at 30 °C for 30 min, and the enzyme activity of 0.1 ml of the insertion mixture was subsequently determined as described previously (40). The product of each assay was then analyzed as published elsewhere (44).

RESULTS AND DISCUSSION

The His-tag ΔnifH MoFe Protein Is an $\alpha_2\beta_2$ Tetramer—Using the previously described method (21), up to 200 mg of His-tag Δ*nifH* MoFe protein/200 g of cells of *A. vinelandii* DJ1165 was purified after one step. This is a 10-fold yield increase compared with that of the conventional purification procedure (10), which was essential for subsequent extensive catalytic and biophysical characterization of this protein.

Fig. 1 shows that the purified His-tag Δ*nifH* MoFe is an $\alpha_2\beta_2$

TABLE I
Metal contents of purified MoFe proteins

Metal	MoFe protein					
	Wild type		Δ*nif*B		Δ*nif*H	
	mol metal/ mol protein	%	*mol metal*/ mol protein	%	*mol metal*/ mol protein	%
Mo	2.2 ± 0.2	100	>0.1		>0.1	
Fe	32.0 ± 1.5	100	18.1 ± 1.9	57	18.6 ± 2.2	58

tetramer, as was described of the non-His-tag version of the Δ*nifH* MoFe protein from the *A. vinelandii* strain DJ54 (10). It has been reported that FeMoco-deficient MoFe protein in DJ54 crude extracts ran well above the position of wild-type MoFe protein on native gels. This was interpreted as a result of loose association of this mutant protein with another protein that was subsequently lost during the long purification procedure (9, 10). However, even with our fast purification procedure, we were not able to detect any protein, which was associated with the purified His-tag Δ*nifH* MoFe protein (Fig. 1, *lane 6*). It is worth mentioning that there is a significant difference between the subunit composition of the His-tag and non-His-tag versions of the Δ*nifB* MoFe proteins of *A. vinelandii.* In contrast to the $\alpha_2\beta_2\gamma_2$ hexamer of Δ*nifB* MoFe protein of *A. vinelandii* UW45 (16, 21), the $\alpha_2\beta_2$ tetrameric His-tag Δ*nifB* MoFe protein of *A. vinelandii* DJ1143 does not contain an additional γ subunit (Ref. 21 and Fig. 1, *lane 4*). Interestingly, although γ, not regulated by *nif* genes, is believed to mediate the insertion of the FeMoco into the FeMoco-deficient MoFe protein (15), the His-tag Δ*nifB* MoFe protein was found to be almost fully reconstituted after the addition of isolated FeMoco in *N*-methylformamide and was therefore considered catalytically active (21). The Δ*nifB* MoFe protein produced by *Klebsiella pneumoniae* also exists as an $\alpha_2\beta_2\gamma_2$ hexamer (12–14), and the additional γ subunit of this organism has been identified as the *nifY* gene product (13, 14). The protein NifY is also present in *A. vinelandii*, although it was known to be different from γ. Both NifY and γ are expressed at very low levels in *A. vinelandii* (21). A large quantity purification and characterization of NifY and γ will be required to address the remaining questions about the exact function of γ and protein interactions involving γ during nitrogenase biosynthesis.

The P-cluster Features of ΔnifH MoFe Protein Are Different from Those of ΔnifB MoFe Protein—Table I shows that isolated His-tag Δ*nifH* MoFe protein contains 18.6 mol of Fe/mol of protein and no detectable molybdenum. The analysis of isolated His-tag Δ*nifB* MoFe protein reveals a metal content almost identical to that of His-tag Δ*nifH* MoFe. The iron content of both mutant proteins, which is around 60% that of wild-type MoFe protein, and the absence of molybdenum in both matches previously described results of presumably P-cluster-containing but FeMoco-deficient MoFe proteins (10, 16, 21). The FeMoco deficiency of His-tag Δ*nifH* and Δ*nifB* MoFe protein is confirmed by the absence of the well characterized S = 3/2 EPR signal, which arises from the FeMoco center of wild-type MoFe protein (Fig. 2, *trace 1*).

Despite the presumably identical cofactor content, Δ*nifH* MoFe and Δ*nifB* MoFe protein are clearly distinguishable by color. Isolated Δ*nifH* MoFe protein has a light brown color, in contrast to the previously described reddish brown color of the Δ*nifB* MoFe protein (21). The apparent differences in color to the eye are consistent with observed differences in the visible range absorption spectra (Fig. 3). The spectrum of Δ*nifB* MoFe protein shows a broad shoulder in the ~475–575-nm range, in contrast to that of the Δ*nifH* MoFe protein, which is essentially featureless in the entire visible region. The difference of the colors and absorption spectra of these two proteins indicates a possible difference between their P-clusters in terms of structure or oxidation state. As shown in Fig. 2 (*trace 2*), isolated His-tag Δ*nifB* MoFe protein exhibits a S = 1/2 EPR signal that is recognized in the g ≈ 2 region and integrated to 0.22 spin/MoFe protein. This signal has been described previously (10,

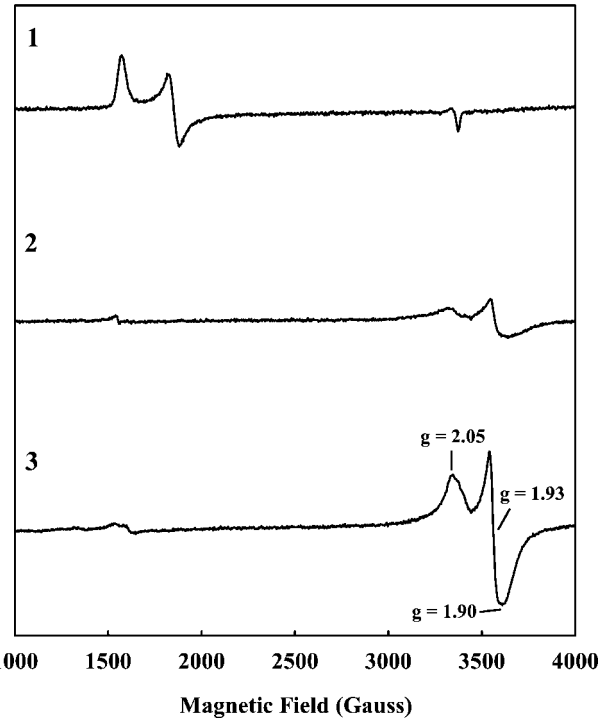

FIG. 2. **EPR spectra of dithionite-reduced wild-type (*1*), Δ*nifB* (*2*), and Δ*nifH* (*3*) MoFe proteins.** The protein concentration was 10 mg/ml. The spectra were measured as described under "Experimental Procedures."

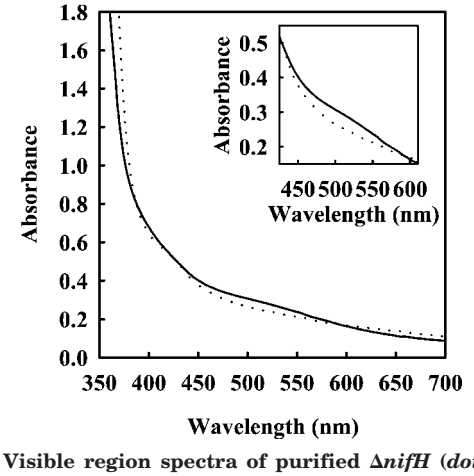

FIG. 3. **Visible region spectra of purified Δ*nifH* (*dotted line*) and Δ*nifB* (*solid line*) MoFe protein.** Spectra are shown from 350 to 700 nm. The inset focuses on the region between 425 and 610 nm. The samples (10 mg/ml protein) were prepared as described under "Experimental Procedures."

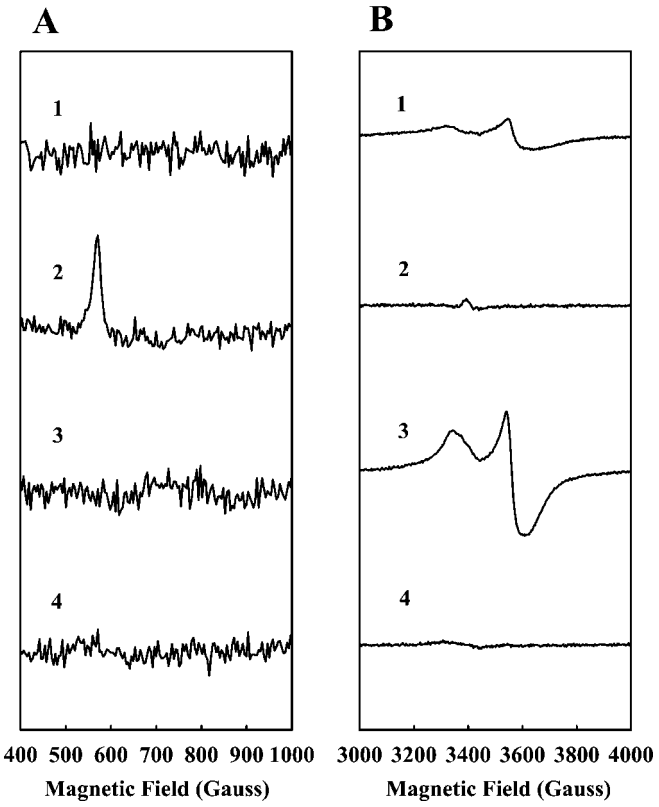

FIG. 4. **Parallel (*A*)- and perpendicular (*B*)-mode EPR spectra of dithionite-reduced and IDS-oxidized Δ*nifB* (*1* and *2*) and Δ*nifH* (*3* and *4*) MoFe protein.** Dithionite-reduced (*1* and *3*) and IDS-oxidized (*2* and *4*) EPR samples (10 mg/ml protein) were prepared and measured as described under "Experimental Procedures." The perpendicular-mode EPR signal in the g ≈ 2 region reappears upon re-reduction of the oxidized sample by sodium dithionite (21). In addition, the g = 11.8 parallel mode EPR signal of the P^{2+} state of the P-cluster was not generated upon oxidation of the Δ*nifH* MoFe protein with methylene blue or ferricyanide (data not shown). The redox potentials of methylene blue ($E^{o\prime}$ = +0.01V) and ferricyanide ($E^{o\prime}$ = +0.452 V) are more positive than that of IDS ($E^{o\prime}$ = −0.125 V).

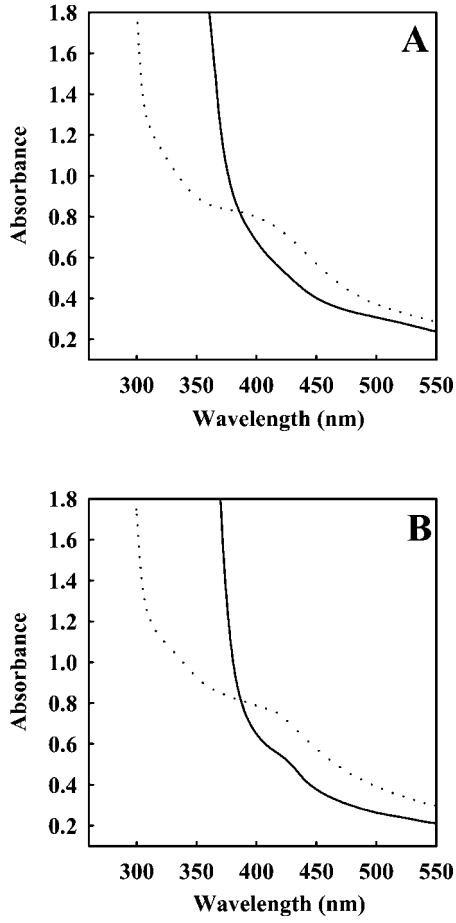

FIG. 5. **UV-visible spectra of Δ*nifB* (*A*) and Δ*nifH* (*B*) MoFe protein.** Spectra are shown from 260 to 550 nm in the dithionite-reduced (*solid line*) and IDS-oxidized state (*dotted line*). The samples (10 mg/ml protein) were prepared as described under "Experimental Procedures."

12, 19, 21, 49) and was interpreted as a very minor species of the P-cluster population (21). The origin of this signal could be explained by the presence of either a P-cluster precursor that is not fully processed (21, 49) or a P-cluster in a state that is more oxidized or reduced than the dithionite-reduced P^N state (10, 19). The identical S = 1/2 EPR signal in the g ≈ 2 region is also present in the His-tag Δ*nifH* MoFe protein sample (Fig. 2, *trace 3*). However, in this case the signal is much stronger and integrated to 0.7 spin/MoFe protein. This is the highest value that has ever been described for this signal and may be the result of the improved protein purification method that helps to prevent protein degradation or destruction of the metal clusters. If the S = 1/2 EPR signal in the g ≈ 2 region arises from a P-cluster precursor, then it should be a major component of the His-tag Δ*nifH* MoFe protein.

The IDS-oxidized ΔnifH MoFe Protein Does Not Show Features of the P^{2+} State of the P-cluster—The P^N state of the P-cluster of wild-type and His-tag Δ*nifB* MoFe proteins can be two-electron-oxidized to the P^{2+} state by IDS (21). This state can be recognized by a g = 11.8 signal observed in the parallel mode EPR (21, 50, 51). Mössbauer data indicate that the "P-cluster" of the isolated Δ*nifH* MoFe protein is in a more oxidized state than that of the Δ*nifB* MoFe protein (a detailed analysis will follow in a later report). If the Δ*nifH* MoFe protein contains a more oxidized P-cluster than that of the Δ*nifB* MoFe protein, it should show the P^{2+} EPR signal upon IDS oxidation.

Fig. 4*A* (*traces 1* and *2*) shows the appearance of the expected g = 11.8 parallel mode EPR signal, and Fig. 4*B* (*traces 1* and *2*) shows the concurrent disappearance of the S = 1/2 perpendicular mode EPR signal in the g ≈ 2 region after the oxidation of the P-cluster of the Δ*nifB* MoFe protein from the P^N to the P^{2+} state by IDS. The g = 11.8 parallel mode EPR signal cannot be observed in the case of the IDS-oxidized Δ*nifH* MoFe protein (Fig. 4*A*, *trace 4*). However, the disappearance of the S = 1/2 perpendicular mode EPR signal (Fig. 4*B*, *traces 1* and *2*) and the simultaneous increase of the absorbance in the visible region around 420 nm (Fig. 5*B*) are evidences for the oxidation of a cluster. An identical absorbance increase at 420 nm was observed in the case of the IDS-oxidized Δ*nifB* MoFe protein (Fig. 5*A*). These results show that the Δ*nifH* MoFe protein, like the Δ*nifB* MoFe protein, can be oxidized by IDS. However, IDS-oxidized Δ*nifH* MoFe protein does not show the expected features of the P^{2+} state, indicating the presence of a possible structurally different cluster from the known P-cluster structure.

Reduced Fe Protein Cannot Transfer Electrons to the IDS-oxidized ΔnifH MoFe Protein—The IDS-oxidized Δ*nifB* MoFe protein in its P^{2+} state can be reduced to the P^{1+} state through a MgATP-dependent one-electron transfer from the $[4Fe\text{-}4S]^{+1}$ state of the Fe protein (21). The P^{1+} state of the P-cluster can be recognized by a rhombic signal in the perpendicular mode EPR with g values of 2.05, 1.94, and 1.81 at pH 7.4 (21, 52).

Fig. 6*A* shows that the parallel mode P^{2+} EPR signals of the sample with the oxidized Δ*nifB* MoFe protein alone (Fig. 6*A*,

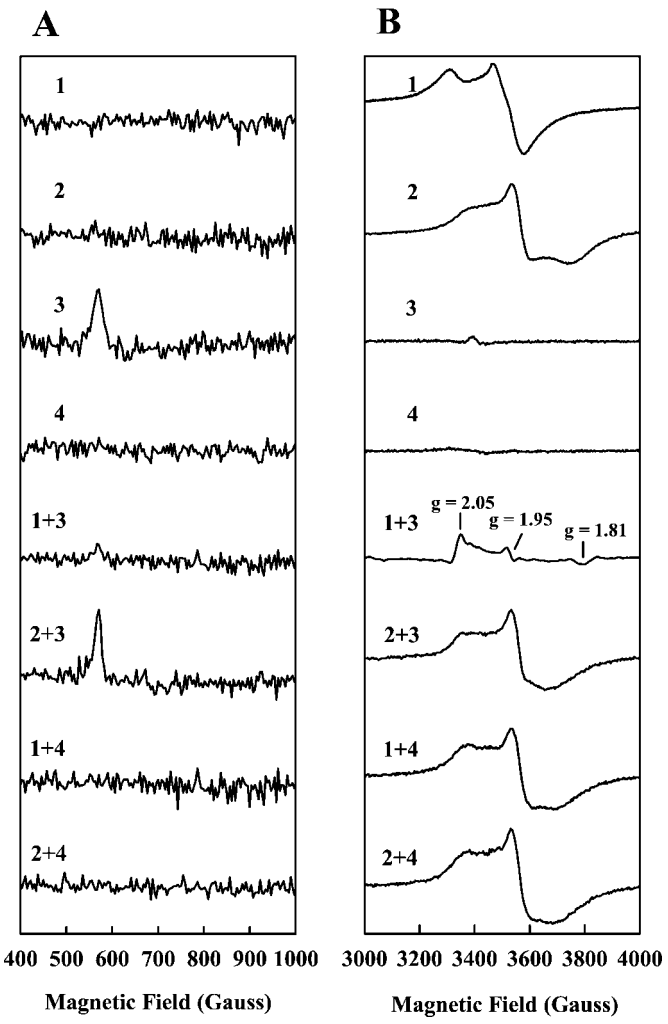

FIG. 6. **Parallel (*A*)- and perpendicular (*B*)-mode EPR spectra of reductant-free nitrogenase turnover samples of IDS-oxidized Δ*nifB* and Δ*nifH* MoFe protein incubated with [4Fe-4S]$^{1+}$ Fe protein.** Spectra shown are: *1*, [4Fe-4S]$^{+1}$ Fe protein + MgATP; *2*, [4Fe-4S] $^{+1}$ Fe protein + MgADP; *3*, IDS-oxidized Δ*nifB* MoFe protein; *4*, IDS-oxidized Δ*nifH* MoFe protein. The concentrations of Fe protein, MoFe protein, MgADP, and MgATP were 14 mg/ml, 25 mg/ml, 3.5 mM, and 3.5 mM, respectively. Parallel (at pH 8.0)- and perpendicular (at pH 7.4)-mode EPR samples were recorded as described under "Experimental Procedures."

trace 3) or the oxidized protein incubated with [4Fe-4S]$^{+1}$ Fe protein and MgADP (Fig. 6*A*, *trace 2 + 3*) are identical, indicating the absence of electron transfer under these conditions. However, there is no parallel-mode P^{2+} EPR signal if the MgADP in the sample is replaced by MgATP (Fig. 6*A*, *trace 1 + 3*), indicating that an electron transfer has occurred and the P^{2+} state is reduced. Fig. 6*B* shows the corresponding perpendicular-mode EPR spectra. The [4Fe-4S]$^{+1}$ Fe protein exhibits the characteristic S = 1/2 EPR signals in the $g \approx 2$ region in the presence of MgATP (Fig. 6*B*, *trace 1*) and MgADP (Fig. 6*B*, *trace 2*). However, the shapes of the signals in these two cases are different, which can be used to distinguish the different Fe protein conformations of these samples (53, 54). During the MgATP-dependent process of electron transfer from the Fe protein to the Δ*nifB* MoFe protein, the P-cluster is reduced from the P^{2+} to the P^{1+} state. Concurrently, the [4Fe-4S]$^{+1}$ cluster of the Fe protein is oxidized to the [4Fe-4S]$^{2+}$ state, which is diamagnetic and, therefore, EPR silent. The disappearance of the S = 1/2 EPR signal, which arises from the [4Fe-4S]$^{+1}$ cluster of the Fe protein in its MgATP-bound conformation, is accompanied by the appearance of the EPR signal which arises from the P^{1+} state of the P-cluster with g values of 2.05, 1.95, and 1.81 (Fig. 6*B*, *trace 1 + 3*). In contrast, the S = 1/2 EPR signals of the MgADP-bound [4Fe-4S]$^{+1}$ Fe protein alone (Fig. 6*B*, *trace 2*) or this conformation of Fe protein incubated with oxidized Δ*nifB* MoFe protein (Fig. 6*B*, *trace 2 + 3*) are identical. Therefore, electron transfer from the Fe protein in the MgADP-bound state to the Δ*nifB* MoFe protein does not occur.

Qualitatively and quantitatively indistinguishable spectra are observed in samples of IDS-oxidized Δ*nifH* MoFe protein incubated with [4Fe-4S]$^{+1}$ Fe protein and either MgADP or MgATP (Fig. 6*B*, *traces 1 + 4* and *2 + 4*). Both spectra are identical to the [4Fe-4S]$^{+1}$ Fe protein in its MgADP-bound conformation in terms of the S = 1/2 EPR signal (Fig. 6*B*, *trace 2*). These data indicate that both MgADP and MgATP are unable to facilitate electron transfer from the [4Fe-4S]$^{+1}$ cluster of the Fe protein to the IDS-oxidized Δ*nifH* MoFe protein. However, the shape of the S = 1/2 EPR signal of the [4Fe-4S]$^{+1}$ Fe protein clearly shows that MgATP is hydrolyzed to MgADP during the incubation (Fig. 6*B*, *trace 1 + 4*). This observation is consistent with the observation of a MgATP hydrolysis activity promoted by purified His-tag Δ*nifH* MoFe protein of 5915 ± 113 nmol MgATP hydrolysis/min/mg of protein, which is ~55% of the activity of wild-type MoFe protein (Table II). Purified His-tag Δ*nifB* MoFe protein shows a similar activity (Table II) and was previously considered to be catalytically active (21). It has been reported that Δ*nifH* MoFe protein of *A. vinelandii* DJ54 was not able to facilitate MgATP hydrolysis by complex formation with the Fe protein to a significant extent (10). However, damages of the fragile mutant protein during the described laborious and time-consuming purification method might be the cause of the loss of the activity of the protein. Despite their abilities to hydrolyze MgATP, the FeMoco-deficient His-tag Δ*nifH* and Δ*nifB* MoFe proteins are not able to demonstrate any substrate-reducing activities, which can be measured by H_2 evolution, C_2H_2 reduction, and the N_2 fixation assays (Table II).

*The Fe Protein Forms a Normal Complex with the Δ*nifH* MoFe Protein*—The chelation assay is another way to study interaction between the Fe protein and the MoFe protein. The binding of MgATP to the [4Fe-4S]$^{+1}$ Fe protein induces a conformational change that involves the contraction of the protein (44, 55–57). Binding of two molecules of MgADP to the state of the Fe protein causes a different, less dramatic conformational change that does not involve a global change in the protein radius of gyration (57). Fig. 7 shows that this reaction can be easily monitored using a chelation assay based on the fact that in the absence of MgATP (or the presence of MgADP) the [4Fe-4S]$^{1+}$ is resistant to chelation by bathophenanthroline disulfonate, whereas in the presence of MgATP, iron is rapidly removed from the protein (58, 59). Once the [4Fe-4S]$^{1+}$ Fe protein is in its MgATP conformation, it is able to form a very specific complex with the MoFe protein. In this complex, the MoFe protein sequesters the [4Fe-4S]$^{1+}$ cluster of the Fe protein, thereby protecting it from chelation (55, 58). Fig. 7, *A–C*, show that there are no observed differences between wild-type, Δ*nifH*, and Δ*nifB* MoFe protein in this chelation protection assay, indicating normal complex formation between the MoFe protein and the Fe protein in all cases.

In summary, the oxidized Δ*nifH* MoFe protein is able to form a specific complex with the [4Fe-4S]$^{1+}$ Fe protein and facilitate the hydrolysis of MgATP within this complex. These data indicate that the Δ*nifH* MoFe protein in this study is present in the correct structural conformation and active in promoting MgATP hydrolysis. However, in contrast to the case of the Δ*nifB* MoFe protein, no concurrent oxidation of the [4Fe-4S]$^{1+}$

TABLE II
Comparison of the activities of purified MoFe proteins

Atmosphere	Product	MoFe protein					
		Wild type		Δ*nif*B		Δ*nif*H	
		nmol/min/mg protein	%	nmol/min/mg protein	%	nmol/min/mg protein	%
10% C_2H_2/90% Ar	C_2H_4	1860 ± 87	100	3 ± 1	>1	9 ± 1	>1
100% N_2	NH_3	1002 ± 148	100	0 ± 0	0	0 ± 0	0
100% N_2	H_2	542 ± 47	100	0 ± 0	0	0 ± 0	0
100% Ar	H_2	2417 ± 161	100	0 ± 0	0	0 ± 0	0
100% Ar	P_i	10962 ± 585	100	4750 ± 50	43	5915 ± 113	54

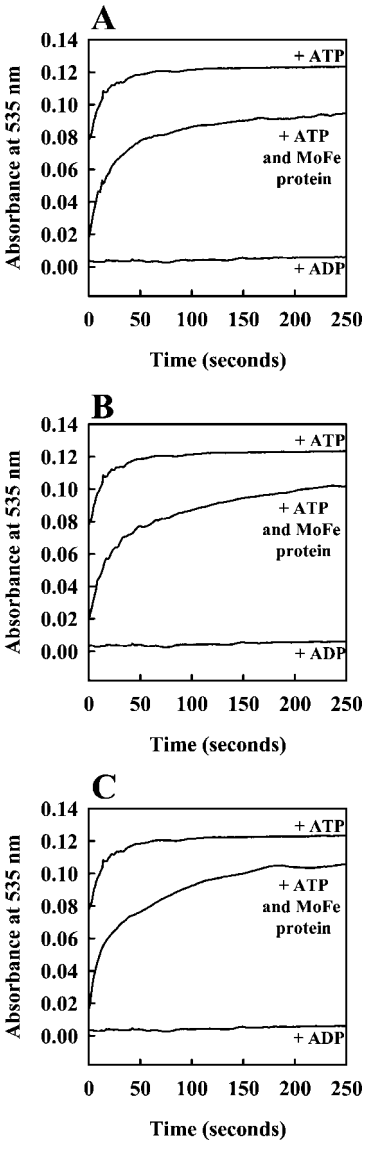

FIG. 7. **Protection of the iron chelation of the [4Fe-4S]$^{1+}$ cluster in the Fe protein by wild type (*A*), Δ*nifB* (*B*), and Δ*nifH* (*C*) MoFe protein.** The formation of the complex between the iron chelator bathophenanthroline disulfonate and the iron from the [4Fe-4S]$^{1+}$ clusters of the Fe proteins was measured at 535 nm in the presence of either MgATP, MgATP and MoFe protein or MgADP. A final concentration of 0.2 mM ADP or ATP and 0.4 mM $MgCl_2$ was used. The MoFe and Fe protein concentrations were 0.13 and 0.08 mg/ml, respectively. Curves obtained in the presence of MgATP and MoFe protein were fitted to single exponential equations over a period of 100 s, giving the observed rate constants of 0.070, 0.068, and 0.069 s^{-1} for the wild-type, Δ*nifB*, and Δ*nifH* MoFe protein, respectively.

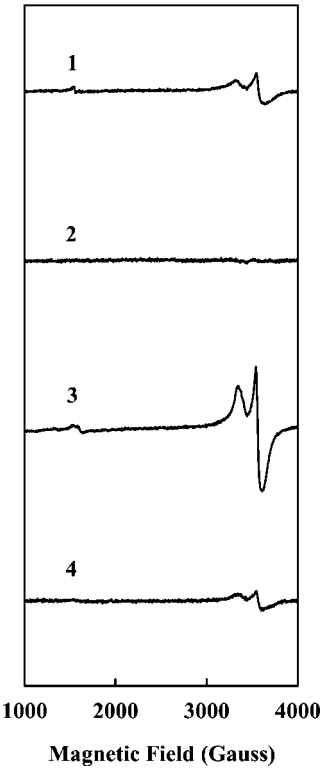

FIG. 8. **EPR spectra of dithionite (*1* and *3*) and Ti(III) citrate (*2* and *4*) reduced Δ*nifB* (*1* and *2*) and Δ*nifH* (*3* and *4*) MoFe protein.** All samples (10 mg/ml protein) were prepared and measured as described under "Experimental Procedures."

cluster of the Fe protein or electron transfer to the oxidized Δ*nifH* MoFe protein is observed. Possible explanations for missing the electron transfer step in the case of this altered protein are either that the P-cluster in this protein exists in a precursor form or the P-cluster is trapped in an unusual conformation or oxidation state that is unable to accept electrons.

The ΔnifH MoFe and ΔnifB MoFe Proteins Can Be Reduced by Ti(III) Citrate—All iron atoms of the P^N state of the MoFe protein, prepared by sodium dithionite reduction, are believed to be in the Fe^{2+} state (21, 60). There is no indication that the P-cluster can be reduced further to a lower oxidation state. Recently it was described that the [4Fe-4S] cluster of the Fe protein could exist not only in the [4Fe-4S]$^{1+}$ state, generated by dithionite reduction, but also in the all-ferrous [4Fe-4S]^0 state, generated by Ti(III) citrate (41, 61). It has been proposed that the [4Fe-4S]$^{2+/0}$ couple, rather than the well established [4Fe-4S]$^{2+/1+}$ couple, is utilized *in vivo* during nitrogenase turnover (42, 62). This finding raised the question as to whether it is also possible to reduce the metal centers of the Δ*nifH* MoFe and Δ*nifB* MoFe protein beyond the dithionite-reduced state as was isolated. The perpendicular mode EPR signals in the $g \approx 2$ region that arise from the dithionite-reduced states of the Δ*nifB* MoFe (Fig. 8, *trace 1*) and Δ*nifH* MoFe protein (Fig. 8, *trace 3*) are greatly diminished upon the reduction with Ti(III) citrate (Fig. 8, *traces 2* and *4*). The

reversibility of this effect (data not shown) in combination with an increase of the absorbance at 420 nm upon Ti(III) citrate addition (data not shown) indicates a reduction of the metal clusters of both FeMoco-deficient MoFe proteins. This behavior could be ascribed to one of the following explanations; (*a*) the P-cluster is reduced to a lower oxidation state than that of P^N or (*b*) a P-cluster precursor that is not fully processed is present in an amount corresponding to the intensity of the EPR signal in the $g \approx 2$ region and is the reason for the described spectroscopic changes.

Activation of ΔnifH MoFe Protein—Previous studies show that FeMoco-deficient MoFe proteins expressed by *A. vinelandii* strains with deletion or mutation of the *nifH* gene cannot be activated simply by adding FeMoco in N-methylformamide (8–10, 18). Several components are required for the insertion of FeMoco into these FeMoco-deficient MoFe proteins, such as the Fe protein, MgATP, γ, and GroEL (9, 11–15, 18). In addition, one, or most likely, several more unidentified components are required for this process, which makes the reconstitution of the proteins difficult. Cell-free extracts of *A. vinelandii* mutant stains like DJ100 (Δ*nifD*) or CA12 (Δ*nifHDK*) are usually supplied as a source of the missing component(s) in activation assays (10, 18). However, it was reported that the maximal activation of purified Δ*nifH* MoFe protein of *A. vinelandii* DJ54 was only around 5% that of the wild-type MoFe protein (10). Our attempt to activate the His-tag Δ*nifH* MoFe protein yielded an activity of 70 nmol of C_2H_2 reduced/min/mg of protein, which also is ~5% wild-type activity. The fact that the full activity of the protein could not be restored can be explained by the failure of FeMoco insertion into the MoFe protein due to the un-optimal assay conditions. However, the presence of a P-cluster precursor or a P-cluster in an unusual conformation or oxidation state that is unable to carry out substrate reduction could also lead to the low activity of the reconstitution assays despite a successful FeMoco insertion. EPR samples of the reconstitution attempts do not show the S = 3/2 EPR signal, which arises from the FeMoco center of the dithionite-reduced wild-type MoFe protein (data not shown). This indicates the possibility of a failed FeMoco insertion, although it does not exclude the possibility that the presence of an unusual P-cluster species has perturbed the reconstituted FeMoco center.

Conclusion—In the current work, an improved method was used to isolate the fragile FeMoco-deficient His-tag Δ*nifH* MoFe protein, which allowed the purification of large amounts of this protein for further studies. In contrast to the results of earlier studies of the non His-tag version of the Δ*nifH* MoFe protein (10), this protein showed MgATP hydrolysis activity as well as the capability of oxidation and reduction based on data obtained from EPR and UV-visible spectroscopy. The failure in detection of these properties of the non-His-tag version of the Δ*nifH* MoFe protein in previous studies could be explained by destruction of the fragile protein during the time-consuming purification procedure. The unusually strong S = 1/2 EPR signal in the $g \approx 2$ region exhibited by the His-tag Δ*nifH* MoFe protein could be ascribed to the presence of a P-cluster precursor or a P-cluster trapped in an unusual conformation or oxidation state in the Δ*nifH* MoFe protein. The presence of a P-cluster species in this mutant protein, which is unable to carry out substrate reduction, would explain the inability of this MoFe protein to restore full activity. It has been proposed previously that during the P-cluster biosynthesis, [4Fe-4S] clusters may be formed separately on the α and β subunit and that they are later combined to form the P-cluster (48). The absence of an intact P-cluster in the protein, which links the α and β subunit of the Δ*nifH* MoFe protein, would explain its high instability and unusual features. The presence of a P-cluster precursor in Δ*nifH* MoFe protein would imply a function of the Fe protein in the P-cluster assembly that has not been described so far. Extended x-ray absorption fine structure and crystallographic investigations will be used to determine the structures of the P-clusters in Δ*nifB* MoFe protein and Δ*nifH* MoFe protein and reveal the origin of the observed characteristics of the Δ*nifH* MoFe protein.

Acknowledgments—We acknowledge Professor Dennis Dean of Virginia Polytechnic Institute and State University for kindly providing the Δ*nifH A. vinelandii* strain DJ1165, Professor Douglas Rees of the California Institute of Technology (Pasadena) for generous support of EPR analysis, Farzad Naderi (University of California, Irvine, program of biotechnology) for technical assistance, and Professor Tom Poulos and Professor Jerry Manning of the University of California, Irvine, for enormous support through the writing of this paper.

REFERENCES

1. Allen, R. M., Chatterjee, R., Madden, M. S., Ludden, P. W., and Shah, V. K. (1994) *Crit. Rev. Biotechnol.* **14,** 225–249
2. Burgess, B. K., and Lowe, D. J. (1996) *Chem. Rev.* **96,** 2983–3011
3. Howard, J. B., and Rees, D. C. (1996) *Chem. Rev.* **96,** 2965–2982
4. Smith, B. E. (1999) *Adv. Inorg. Chem.* **47,** 159–218
5. Rees, D. C., and Howard, J. B. (2000) *Curr. Opin. Chem. Biol.* **4,** 559–566
6. Christiansen, J., Dean, D. R., and Seefeldt, L. C. (2001) *Annu. Rev. Plant Physiol. Plant Mol. Biol.* **52,** 269–295
7. Robinson, A. C., Dean, D. R., and Burgess, B. K. (1987) *J. Biol. Chem.* **262,** 14327–14332
8. Robinson, A. C., Chun, T. W., Li, J.-G., and Burgess, B. K. (1989) *J. Biol. Chem.* **264,** 10088–10095
9. Tal, S., Chun, T. W., Gavini, N., and Burgess, B. K. (1991) *J. Biol. Chem.* **266,** 10654–10657
10. Gavini, N., Ma, L., Watt, G., and Burgess, B. K. (1994) *Biochemistry* **33,** 11842–11849
11. Allen, R. M., Homer, M. J., Chatterjee, R., Ludden, P. W., Roberts, G. P., and Shah, V. K. (1993) *J. Biol. Chem.* **268,** 23670–23674
12. Hawkes, T. R., and Smith, B. E. (1983) *Biochem. J.* **209,** 43–50
13. Homer, M. J., Paustian, T. D., Shah, V. K., and Roberts, G. P. (1993) *J. Bacteriol.* **175,** 4907–4910
14. White, T. C., Harris, G. S., and Orme-Johnson, W. (1992) *J. Biol. Chem.* **267,** 24007–24016
15. Homer, M. J., Dean, D. R., and Roberts, G. P. (1995) *J. Biol. Chem.* **270,** 24745–24752
16. Paustian, T. D., Shah, V. K., and Roberts, G. P. (1990) *Biochemistry* **29,** 3515–3522
17. Ribbe, M. W., Bursey, E. H., and Burgess, B. K (2000) *J. Biol. Chem.* **275,** 17631–17638
18. Ribbe, M. W., Burgess, B. K. (2001) *Proc. Natl. Acad. Sci. U. S. A.* **98,** 5521–5525
19. Ma, L., Brosius, M. A., and Burgess, B. K. (1996) *J. Biol. Chem.* **271,** 10528–10532
20. Musgrave, K. N., Liu, H. I., Ma., L., Burgess, B. K., Watt, G., Hedman, B., and Hodgson, K. O. (1998) *J. Biol. Inorg. Chem.* **3,** 344–352
21. Christiansen, J., Goodwin, P. J., Lanzilotta, W. N., Seefeldt, L. C., and Dean, D. R. (1998) *Biochemistry* **37,** 12611–12623
22. Hawkes, T. R., and Smith, B. E. (1984) *Biochem. J.* **223,** 783–792
23. Allen, R. M., Chatterjee, R., Ludden, P. W., and Shah, V. K. (1995) *J. Biol. Chem.* **270,** 26890–26896
24. Ugalde, R. A., Imperial, J., Shah, V. K., and Brill, W. J. (1984) *J. Bacteriol.* **159,** 888–893
25. Fuller, W. A., Kemp, R. M., Ng, J. C., Hawkes, T. R., and Smith, B. E. (1986) *Eur. J. Biochem.* **160,** 371–377
26. Robinson, A. C., Burgess, B. K., and Dean, D. R. (1986) *J. Bacteriol.* **166,** 180–186
27. Peters, J. W., Fischer, K., and Dean, D. R. (1995) *Annu. Rev. Microbiol.* **49,** 335–366
28. Burgess, B. K. (1990) *Chem. Rev.* **90,** 1377–1406
29. Burgess, B. K. (1993) in *Molybdenum Enzymes, Cofactors, and Model Systems* (Stiefel, E. I., Coucouvanis, D., and Newton, W. E., eds) pp. 144–169, No. 535, American Chemical Society, Washington, D. C.
30. Dean, D. R., and Jacobson, M. R. (1992) in *Biological Nitrogen Fixation* (Stacey, G., Burris, R. H., and Evans, H. J., eds) pp. 763–834, Chapman & Hall, New York
31. Shah, V. K., Rangaraj, P., Chatterjee, R., Allen, R. M., Roll, J. T., Roberts, G. P., and Ludden, P. W. (1997) in *Biological Nitrogen Fixation for the 21st Century* (Elmerich, C., Kondorosi, A., and Newton, W. E., eds) pp. 51–52, Kluwer Academic Publishers, Norwell, MA
32. Newton, W. E. (1992) in *Biological Nitrogen Fixation* (Stacey, G., Burris, R. H., and Evans, H. J., eds) pp. 877–929, Chapman & Hall, New York
33. Smith, B. E., and Eady, R. R. (1992) *Eur. J. Biochem.* **205,** 1–15
34. Hoover, T. R., Imperial, J., Ludden, P. W., and Shah, V. K. (1988) *Biofactors* **1,** 199–205
35. Shah, V. K., Rangaraj, P., Chatterjee, R., Allen, J. R., Roll, J. T., Roberts, G. P., and Ludden, P. W. (1999) *J. Bacteriol.* **181,** 2797–2801
36. Peters, J. W., Stowell, M. H. B., Soltis, S. M., Finnegan, M. G., Johnson, M. K., and Rees, D. C. (1997) *Biochemistry* **36,** 1181–1187
37. Lowe, D. J., Fisher, K., and Thorneley, R. N. F. (1993) *Biochem. J.* **292,** 93–98
38. Jacobson, M. R., Cash, V. L., Weiss, M. C., Laird, N. F, Newton, W. E, and Dean, D. R. (1989) *Mol. Gen. Genet.* **219,** 49–57

39. Bursey, E. H., and Burgess, B. K. (1998) *J. Biol. Chem.* **273,** 16927–16934
40. Burgess, B. K., Jacobs, D. B., and Stiefel, E. I. (1980) *Biochim. Biophys. Acta* **614,** 196–209
41. Bursey, E. H., and Burgess, B. K. (1998) *J. Biol. Chem.* **273,** 29678–29685
42. Angove, H. C., Yoo, S. J., Burgess, B. K., and Münck, E. (1997) *J. Am. Chem. Soc.* **119,** 8730–8731
43. Angove, H. C., Yoo, S. J., Münck, E., and Burgess, B. K. (1998) *J. Biol. Chem.* **273,** 26330–26337
44. Gavini, N., and Burgess, B. K. (1992) *J. Biol. Chem.* **267,** 21179–21186
45. Corbin, J. L. (1984) *Appl. Environ. Microbiol.* **47,** 1027–1030
46. Fiske, C. H., amd Subbarow, Y. (1952) *J. Biol. Chem.* **66,** 325–400
47. Clark, L. J., and Axley, J. H. (1955) *Anal. Biochem.* **27,** 2000
48. Van de Bogart, M., and Beinert, H. (1967) *Anal. Biochem.* **20,** 325–334
49. Blanchard, C. Z., and Hales, B. J. (1996) *Biochemistry* **35,** 472–478
50. Surerus, K. K., Hendrich, M. P., Christie, P. D., Rottgardt, D., Orme-Johnson, W. H., and Münck, E. (1992) *J. Am. Chem. Soc.* **114,** 8579–8590
51. Pierik, A. J., Wassink, H., Haaker, H., and Hagen, W. R. (1993) *Eur. J. Biochem.* **212,** 51–61
52. Tittsworth, R. C., and Hales, B. J. (1993) *J. Am. Chem. Soc.* **115,** 9763–9767
53. Zumft, W. G., Palmer, G., and Mortenson, L. E. (1973) *Biochim. Biophys. Acta* **292,** 413–421
54. Zumft, W. G., Mortenson, L. E., and Palmer, G. (1973) *Eur. J. Biochem.* **46,** 525–535
55. Schindelin, H., Kisker, C., Schlessman, J. L., Howard, J. B., and Rees, D. C. (1997) *Nature* **387,** 370–376
56. Seefeldt, L. C., and Dean, D. R. (1997) *Acc. Chem. Res.* **30,** 260–266
57. Chen, L., Gavini, N., Tsuruta, H., Eliezer, D., Burgess, B. K., Doniach, S., and Hodgson, K. O. (1994) *J. Biol. Chem.* **269,** 3290–3294
58. Walker, G. A., and Mortenson, L. E. (1974) *Biochemistry* **13,** 2382–2388
59. Deits, T. L., and Howard, J. B. (1989) *J. Biol. Chem.* **264,** 6619–6628
60. Zimmerman, R., Münck, E., Brill, W. J., Shah, V. K., Henzl, M. T., Rawlings, J., and Orme-Johnson, W. H. (1978) *Biochim. Biophys. Acta* **537,** 185–207
61. Watt, G. D., and Reddy, K. R. N. (1994) *J. Inorg. Biochem.* **53,** 281–294
62. Erickson, J. A., Nyborg, A., C., Johnson, J. L., Truscott, S. M., Gunn, A., Nordmeyer, F. R., and Watt, G. D. (1999) *Biochemistry* **38,** 14279–14285